Interaction of Cardiotoxins with Membranes: A Molecular Modeling Study

Roman G. Efremov, Pavel E. Volynsky, Dmitry E. Nolde, Peter V. Dubovskii, and Alexander S. Arseniev
M. M. Shemyakin & Yu. A. Ovchinnikov Institute of Bioorganic Chemistry, Russian Academy of Sciences, Moscow V-437, 117997 GSP, Russia

ABSTRACT Incorporation of β-sheet proteins into membrane is studied theoretically for the first time, and the results are validated by the direct experimental data. Using Monte Carlo simulations with implicit membrane, we explore spatial structure, energetics, polarity, and mode of insertion of two cardiotoxins with different membrane-destabilizing activity. Both proteins, classified as P- and S-type cardiotoxins, are found to retain the overall "three-finger" fold interacting with membrane core and lipid/water interface by the tips of the "fingers" (loops). The insertion critically depends upon the structure, hydrophobicity, and electrostatics of certain regions. The simulations reveal apparently distinct binding modes for S- and P-type cardiotoxins via the first loop or through all three loops, respectively. This rationalizes an earlier empirical classification of cardiotoxins into S- and P-type, and provides a basis for the analysis of experimental data on their membrane affinities. Accomplished with our previous simulations of membrane α-helices, the computational method may be used to study partitioning of proteins with diverse folds into lipid bilayers.

INTRODUCTION

Delineation of physical principles that drive protein insertion into lipid bilayers is of significant biological relevance. To date, remarkable progress has been made in experimental studies of transmembrane (TM) proteins; several three-dimensional (3D) structures of them have been solved to an atomic resolution (White and Wimley, 1999). Moreover, a number of computer simulations of TM proteins and their individual membrane-binding components have been reported (Forrest and Sansom, 2000; Tieleman et al., 2001). Unlike the membrane-spanning proteins, atomic-scale structural information about the peripheral membrane proteins is scarce. Functions of some of these proteins require them to be folded in an aqueous environment and also be capable of inserting themselves into membranes. Studies of such "ubiquitous" molecules provide an opportunity to examine the determinants of an insertion event. Unfortunately, the experimental analysis is seriously hampered by difficulties in preparation of suitable samples containing these proteins in the membrane-bound state. Their high-resolution structures obtained so far reveal the only binding motif: an amphiphilic α-helix either lying on the bilayer surface or partly immersed into the hydrophobic core (White and Wimley, 1999; Shai, 1999). Based on these structural data, a number of successful molecular modeling studies of interactions between α-helices and membrane interface have been reported (Forrest and Sansom, 2000; Tieleman et al., 2001).

Do the peripheral membrane proteins possess other types of binding motifs? Certainly; there is a wealth of experimental evidence for this. However, the corresponding high-resolution data have been missing until recent elaboration of the 3D structure of cytotoxin II (CX2) from *Naja oxiana* in dodecylphosphocholine (DPC) micelles (Dubovskii et al., 2001). CX2 belongs to the family of so-called "three-finger" (or "three-loop") proteins which, apart from cardiotoxins (cytotoxins, CTXs), includes snake neurotoxins and some CTX-like basic proteins. Known solution and crystal 3D structures of CTXs show that these small (60–62 amino acid residues) molecules reveal common β-sheet fold, but diverse biological activities (Kumar et al., 1997). Unlike other representatives of the family, CTXs bind to cell membranes; they are capable of damaging a wide variety of cells presumably by perturbing the structure of lipid bilayers (Vincent et al., 1978; Gatineau et al., 1990). Despite the similarity of structures, number of basic residues, and so forth, the ability to destabilize a bilayer differs for various CTXs (Bougis et al., 1983). Depending on these characteristics, the toxins are subdivided into two distinct types, i.e., S- and P-type CTXs (Chien et al., 1994). They both interact with anionic phospholipids, but only P-type CTXs bind to zwitterionic ones (Chien et al., 1994; Sue et al., 1997). Earlier experiments along with the analysis of the 3D structure of CX2 in micelles imply that the toxins protrude into membranes via the hydrophobic tips of their β-sheet loops—the feature that distinguishes CTXs from other peripheral membrane proteins, which bind through the amphipathic α-helices.

Overall, experimental studies have commonly found that CTXs' insertion and, hence, their functional specificity is determined by structural and hydrophobic properties of the three-finger loops (Kumar et al., 1997). For β-structural proteins the mechanisms of binding to membranes are not well understood, and the related topics are poorly covered in the literature. Moreover, no attempts of theoretical analysis of the molecular events accompanying interactions of β-sheet proteins with lipid bilayers have been reported so

Submitted December 21, 2001, and accepted for publication February 28, 2002.

Address reprint requests to Dr. Roman G. Efremov, 16/10 Ul. Miklukho-Maklaya, Moscow 117997, Russia. Tel.: 7-095-335-5155; Fax: 7-095-335-5033; E-mail: efremov@nmr.ru.

0006-3495/02/07/144/10 $2.00

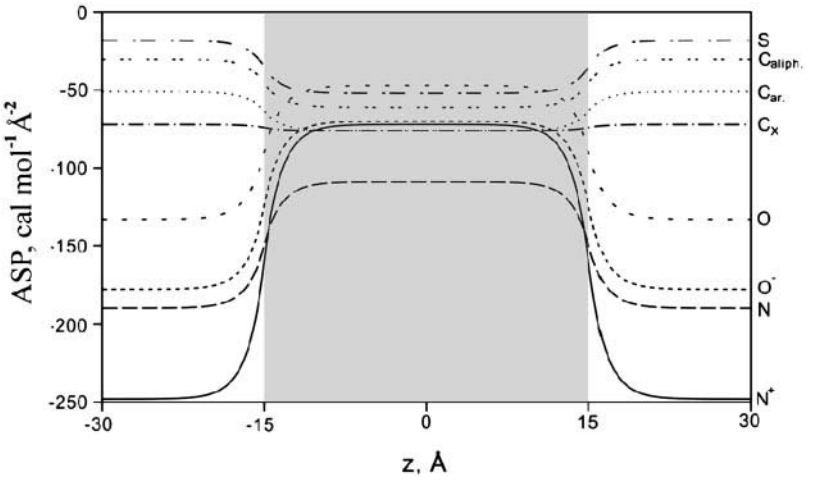

FIGURE 1 The values of atomic solvation parameters versus coordinate z for different atom types used in the membrane model. The atom types are C_{ali}, aliphatic carbon; C_{aro}, aromatic carbon; C_{het}, carbon atoms bonded to any heteroatom (including those in aromatic rings); S, sulfur; O and O^-, uncharged and charged oxygen, respectively; N and N^+, uncharged and charged nitrogen, respectively. Nonpolar layer of the membrane is shown in gray.

far. Progress in this field will lead to important developments in our concepts of how the partition of proteins into membranes may proceed. An intriguing challenge of a realistic physical description of this process is provided by the 3D structure of CX2 in membrane-like media (Dubovskii et al., 2001), together with the theoretical approach, which has been successfully applied to membrane α-helices (Efremov et al., 1999a; Nolde et al., 2000). To implement this, we investigate spatial structure, energetics, and mode of membrane binding of two CTXs with different abilities to destabilize the bilayer, CX2 of P-type and cytotoxin I from *Naja atra* (CX1) of S-type (Jahnke et al., 1994), via Monte Carlo (MC) simulations. The computational results are comparable to experimentally derived parameters and give a coherent picture of the CTX-membrane interactions. The approach may appear to be an oversimplification compared to the full-atom membrane model (e.g., Berneche et al., 1998; La Rocca et al., 1999; Forrest and Sansom, 2000; Tieleman et al., 2001); nevertheless, it gives a picture fully consistent with the available experimental data, and thus may be used for relatively fast tests of membrane insertion for a wide class of membrane proteins.

METHOD OF CALCULATION

The membrane model

The membrane was represented by a "hydrophobic slab" described by an effective solvation potential (Fig. 1). This was done using atomic solvation parameters (ASP) for gas-cyclohexane and gas-water transfer, which mimic the hydrophobic membrane core, lipid-water interface, and aqueous solution (Nolde et al., 2000). All-atom potential energy function for protein was taken in the form $E_{total} = E_{ECEPP/2} + E_{solv} + E_{\Delta\psi}$. The term $E_{ECEPP/2}$ includes van der Waals, torsion, electrostatic, hydrogen, and disulfide bonding contributions (Némethy et al., 1983). E_{solv} is the solvation energy:

$$E_{solv} = \sum_{i=1}^{N} \Delta\sigma_i \, ASA_i \qquad (1)$$

where ASA_i and $\Delta\sigma_i$ are accessible surface area (ASA) and ASP of atom i, respectively, and N is the number of atoms. The values of ASPs were taken from Efremov et al. (1999b). Interaction of the protein with both aqueous and membrane environments is given by Eq. 2, where $\Delta\sigma_i$ depends on the z-coordinate of atom i (axis Z is normal to the membrane plane). Assuming that apart from the water-membrane interfaces the values of ASPs correspond to those either for bulk water or cyclohexane (Fig. 1), we propose that:

$$\Delta\sigma_i(z) =$$

$$\begin{cases} \Delta\sigma_i^{mem} - 0.5 \cdot (\Delta\sigma_i^{mem} - \Delta\sigma_i^{wat}) \cdot e^{(|z|-z_0)/\lambda}, & \text{if} \quad |z| < z_0 \\ \Delta\sigma_i^{wat} + 0.5 \cdot (\Delta\sigma_i^{mem} - \Delta\sigma_i^{wat}) \cdot e^{-(|z|-z_0)/\lambda}, & \text{if} \quad |z| \geq z_0 \end{cases} \qquad (2)$$

where $\Delta\sigma_i^{mem}$ and $\Delta\sigma_i^{wat}$ are ASP values for the type i atom in aqueous (*wat*) or nonpolar (*mem*) environments, respectively; z_0 is a half-width of the membrane (i.e., the hydrophobic layer is restricted by the planes given by the equation $z = z_0$); $D = 2z_0$ is the membrane thickness (30 Å); and λ is a characteristic half-width of the water-membrane interface (in this study $\lambda = 1.5$ Å). We should note that, although the ASP-based model gives results that are in good agreement with NMR data on proteins in micelles, it does not describe the layer of negatively charged headgroups of lipids. Its influence is taken into account (at least partially) by introducing the term $E_{\Delta\psi}$, which reflects the effect of TM voltage ($\Delta\psi$) (La Rocca et al., 1999):

$$E_{\Delta\psi} = (F\Delta\psi/D)\sum_{i=1}^{N} q_i z_i \qquad (3)$$

where q_i and z_i are partial charge and coordinate z of atom i, and F is Faraday's constant. For $|z_i| > z_0$, $\psi(z) = \text{const}$. $E_{\Delta\psi}$ was used only in one MC run, to model interaction of CX2 with anionic phospholipid bilayer.

Simulation protocol

Coordinates of CX1, major and minor forms of CX2 in aqueous solution, and CX2 in DPC micelles (starting structure for MC simulations), were taken from the Protein Data Bank (Berman et al., 2000) entries 2CDX, 1CB9, 1CCQ, and 1FFJ, respectively. The proteins' conformational space was explored via MC search in torsion angle space using the modified FANTOM program (von Freyberg and Braun, 1991). Unless otherwise stated, the starting structures were arbitrary placed in the aqueous phase. To change during the simulation orientation of proteins with respect to the membrane, fragments of 20 dummy residues were attached to their N-termini. The number of dummy residues is determined by the membrane

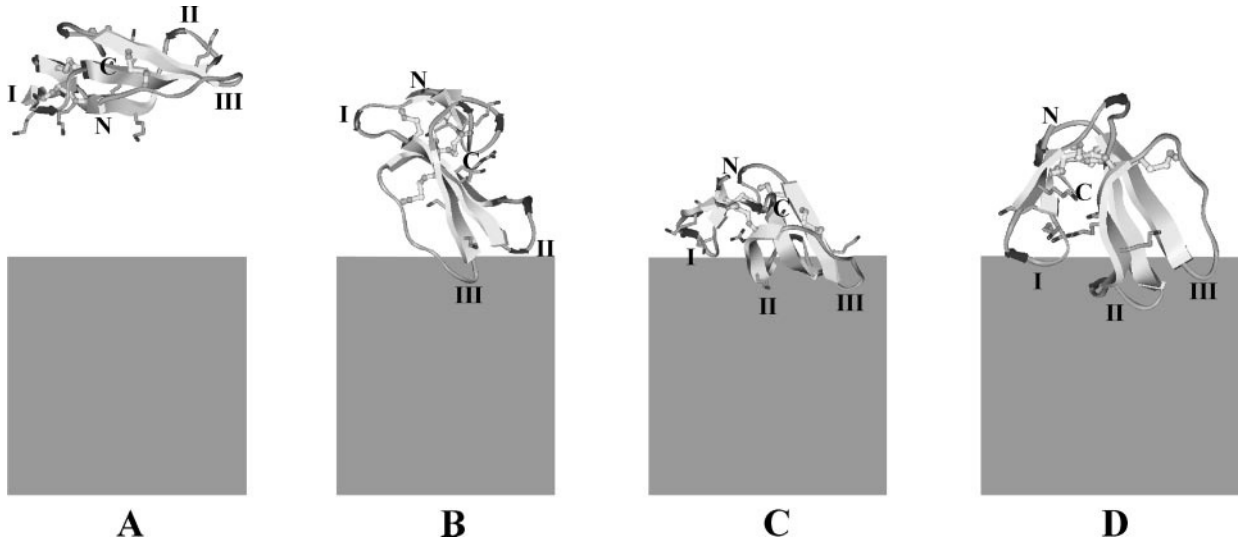

FIGURE 2 Results of Monte Carlo simulation of cytotoxin II from *Naja oxiana* (CX2) in membrane-mimic media. Starting (*A*), intermediate (*B* and *C*), and lowest-energy (*D*) states. β-Sheets and β-turns are displayed with large and small ribbons, respectively. The toxin's loops are marked with roman numerals. Disulfides and side chains of Lys and Arg residues are given respectively in stick-and-ball and stick representation. N- and C-termini are marked with "N" and "C". The nonpolar layer of membrane is shown in gray.

half-width and the protein size. These "virtual" residues do not contribute to the energy of the system. The first atom of the N-terminal dummy residue was always placed in the center of the hydrophobic layer with coordinates (0, 0, 0). All dihedral angles were sampled, except angles ω in "real" residues. The step of variation of each dihedral was chosen randomly in the range $-180° \div 180°$. Nonbond interactions were truncated with a spherical cutoff of 25 Å. Electrostatic interactions were treated with distance-dependent dielectric permeability $\epsilon = 4 \times r$. In our opinion, more sophisticated schemes for treatment electrostatics (e.g., solution of the Poisson-Boltzmann equation) are too computationally demanding for exhaustive MC search coupled with energy minimizations. The choice of the dielectric screening model was discussed in detail elsewhere (Efremov et al., 1999b). Before MC simulations, the structures were subjected to 100 cycles of conjugate gradient minimization. Acceptance of the MC-states was done according to the Metropolis criterion (Metropolis et al., 1953). To cross the energy barriers between local minima an adaptive-temperature schedule protocol (von Freyberg and Braun, 1991) was used. In the beginning of the MC search for CX2 (first 5×10^3 MC steps), a number of distance restraints obtained from NMR experiments in DPC micelles (Dubovskii et al., 2001), was applied. Then several consecutive MC runs (5×10^3 steps each) with different seed numbers and sampled 5, 3, 2, 1 randomly chosen torsion angles were performed without restraints. At each MC step the structures were minimized via 50–120 conjugate gradient iterations. In each run the initial conformation was the lowest-energy one found in previous runs. In total, $\sim 2.5 \times 10^4$ MC steps were performed for all proteins in one complete MC simulation.

To address the convergence problem in the MC search, several independent simulations with different seed numbers were carried out for each protein. In the case of the major form of CX2, three different starting structures (arbitrary placed in water layers) were used, while for its minor form and CX1 two independent starts were used (see below). It is important to note that the sets of low-energy states obtained for each protein in all the simulations are quite similar in total energy and its individual terms, structure, and mode of membrane binding. This provides strong reasons to believe that the essential sampling of the toxins' conformational space was reached in each MC simulation.

Analysis of simulation results and polarity properties of cardiotoxins

Resulting states of CTXs were analyzed using the following parameters calculated both for the whole protein and for individual residues: total energy; energy of interaction with nonpolar membrane core (E_{np}), interface (E_{int}), and water (E_{pol}); disposition with respect to membrane; and secondary structure. The ASA-values and secondary structure were assessed using the DSSP program (Kabsch and Sander, 1983). Ribbon diagrams of the molecules were produced with the MOLMOL software (Koradi et al., 1996). The molecular hydrophobicity potential (MHP) created by protein atoms on the solvent-accessible surface was calculated as described earlier (Efremov and Vergoten, 1995). The scores *S*, which characterize the "quality" of residues' environment in 3D structure, were calculated using the program Profiles 3D (Bowie et al., 1991). Environmental classes (EC) of residues were defined as follows: "E," exposed to solvent; "P1", "P2," partially exposed to solvent, nonpolar and polar protein surrounding, respectively; "B1", "B3," buried, nonpolar and polar protein surrounding, respectively (Bowie et al., 1991). Rough measure of values *S* in the membrane-embedded state was done as follows. If residue *i* interacts neither with the hydrophobic layer nor with the interface, S_i remains unchanged. Otherwise, the following changes of ECs (and corresponding values of S_i) were accounted: for residues interacting with the hydrophobic membrane core ($E_{np} \neq 0$), initial ECs "E," "P2," and/or "P1" were reassigned to "B1"; for residues interacting with the membrane interface ($E_{int} \neq 0$), reassignments "E" $\rightarrow$ "P1" and "P2" $\rightarrow$ "B3" were done. Other details of the simulations and data analysis were described earlier (Nolde et al., 2000; Efremov et al., 1999a,c).

RESULTS

CX2 binds to model membrane with the tips of three loops

The results of MC simulation of CX2 are presented in Figs. 2-4. In the beginning the molecule was placed in water,

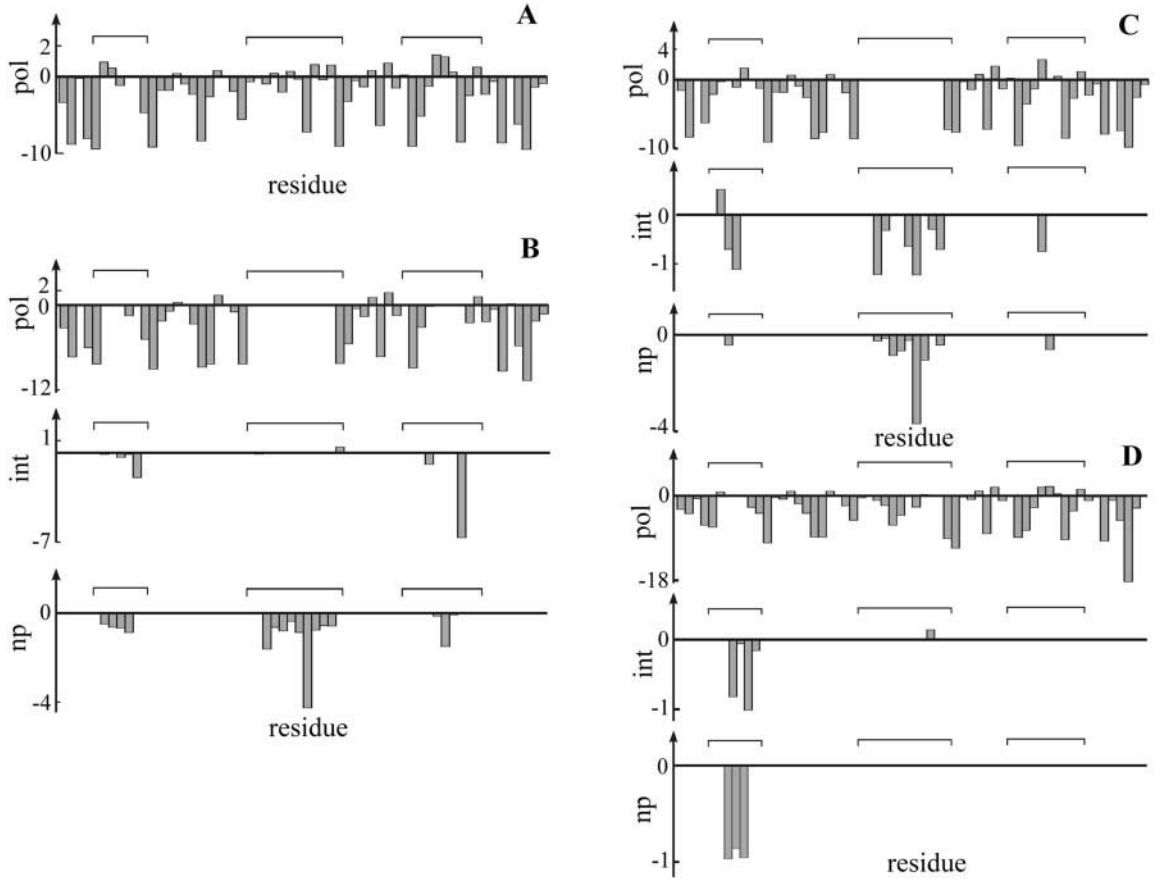

FIGURE 3 Energies of interaction (in kcal/mol) of residues with polar solvent (*pol*), membrane-water interface (*int*), and hydrophobic layer of membrane (*np*). (*A* and *B*) Major form of cytotoxin II from *Naja oxiana* (CX2) in water and membrane, respectively; (*C*) minor form of CX2 in membrane; (*D*) cytotoxin I from *Naja atra* in membrane. The structures in membrane correspond to the lowest-energy states found via Monte Carlo simulations. Positions of loops are indicated with horizontal lines.

outside the membrane (Fig. 2 *A*). After several thousand MC steps, one, two, or all three toxin's loops were found in contact either with the interface or with the hydrophobic layer of the membrane (Fig. 2, *B* and *C*). Subsequent MC simulations resulted in significant decreasing of energy. (Here and thereafter the term "energy" refers to the sum of internal protein energy and the energy of its interaction with heterogeneous membrane-mimic media (E_{solv}), while the energy of the membrane itself is considered to be constant.) Analysis of the low-energy states (Fig. 2 *D*) emphasizes that 1) calculated spatial structure and geometry of insertion are similar to those obtained by NMR in DPC micelles (Dubovskii et al., 2001); 2) CX2 inserts into the membrane with the nonpolar tips of three loops, residues 6–10 (loop I), 24–34 (loop II), and 46–52 (loop III); 3) in the lowest-energy state, the energies of interaction of loops I–III with the hydrophobic layer (E_{np}) and with the interface (E_{int}) are -2.93, -10.27, -1.76 kcal/mol and -2.44, -0.08, -6.88 kcal/mol, respectively (Fig. 3 *B*). The states with similar modes of membrane binding exist in the energy range $\approx$9 kcal/mol; 4) the membrane-embedded protein part is flanked with positively charged Lys and Arg residues: 4, 5, 12, 23, 35, 36, 50. They form a polar "belt" on the protein surface (Fig. 4), which prevents deeper insertion of CX2. Strongest interactions with membrane are characteristic for Lys-35 and -50. Lys-5 and Arg-36 demonstrate weaker binding, while E_{np} and E_{int} for Lys-4, -12, and -23 are negligibly small (Fig. 3 *B*); 5) the states with other geometries of binding (which differ from the lowest-energy ones by E_{np} and/or E_{int}), are higher in energy by $\sim$15 kcal/mol. The above conclusions were made for electrically neutral membranes. To model the interaction of CTXs with anionic phospholipid bilayers, we explored the behavior of CX2 in the presence of negatively charged membrane. A negative charge on one of the surfaces was modeled by introducing the term $E_{\Delta\psi}$ with $\Delta\psi = 100$ mV, as described in Methods. The results of MC simulations exhibit deeper (by 1–2 Å) embedding of loops II and III into the hydrophobic layer, while loop I retains the same membrane-bound state, such as that found in calculations with uncharged ($\Delta\psi = 0$ mV) membrane (data not shown).

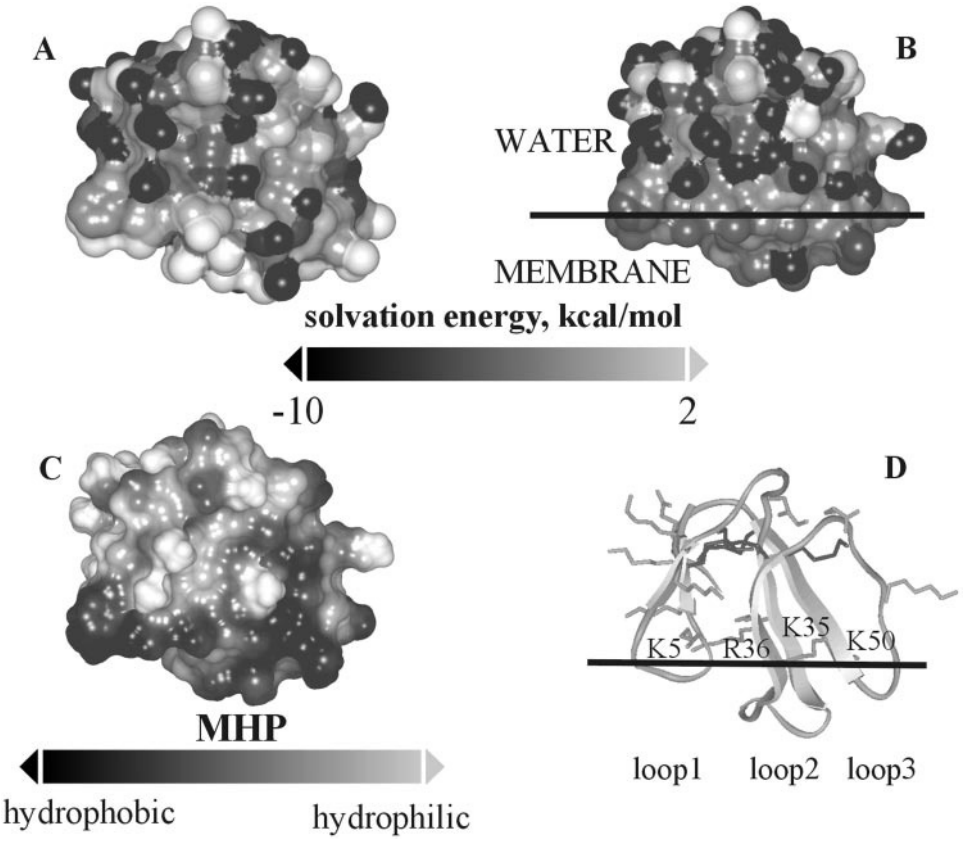

FIGURE 4 Polarity properties of the surface of cytotoxin II from *Naja oxiana* (CX2). (*A* and *B*) Solvation energies (E_{solv}) of CX2 residues in water and membrane-bound state. The values of E_{solv} are shown according to the gray scale from −10 to 2 kcal/mol. (*C*) Molecular hydrophobicity potential (hydrophobic and hydrophilic areas are colored in dark- and light-gray, respectively). All views are given for the same orientation of CX2 (*D*), which is the lowest-energy state found via Monte Carlo simulations. The straight line indicates the membrane-water boundary.

Polarity properties of CX2: the driving force for water → membrane partition

It is commonly accepted that hydrophobic interactions play a dominant role in protein binding to membranes (White and Wimley, 1999). As shown above, to reach the most energetically favorable state CX2 inserts into membrane instead of staying in aqueous solution. Because the structure of CX2 does not significantly change upon insertion, its binding capacity is governed by polarity properties of solvent-exposed residues. These characteristics were estimated using three independent approaches. 1) The accessible surface of the molecule was mapped according to the solvation energy (E_{solv}) in water and in the membrane-water system (Fig. 4, *A* and *B*). The surface regions with negative and positive E_{solv} correspond to favorable and unfavorable interactions with the environment, respectively. In water most of the regions with high E_{solv} are attributed to tips of loops I–III (Fig. 4 *A*). In contrast, insertion into membrane (Fig. 4 *B*) leads to significant decrease of E_{solv} for this region of CX2; 2) folded membrane proteins interact with the acyl chain core of lipid bilayer via their hydrophobic parts, while the polar ones are either on the interface or exposed to water. To delineate these parts, we calculated MHP values (Efremov and Vergoten, 1995) on the surface. As one can see in Fig. 4 *C*, the most hydrophobic zone of CX2 (MHP $>$ 0, dark gray) includes the tips of loops, and there is a polar "belt" (MHP $<$ 0, light gray) created by charged atoms of Lys and Arg. It confines hydrophobic parts of the surface and determines the extent to which CX2 inserts into membrane; 3) the tendency of residues to be in a certain environment (in 3D protein structure, in water, on the interface or inside the membrane) might be expressed in terms of a so-called compatibility score (*S*) between spatial structure and sequence (Bowie et al., 1991). Thus, positive and negative values of *S* indicate favorable and unfavorable environments of a given residue in a given 3D structure. As seen on the plot of *S* versus residue number, the regions of CX2 with negative *S* in water are disposed in the tips of loops (Fig. 5, *solid line*). Burial of CX2 into membrane according to the model considered above leads to significant "improvement" of environments for these residues, and resulting values of *S* are higher than those in water (Fig. 5, *dotted line*). In this case the scores *S* of residues interacting with the nonpolar membrane core and/or with interface were changed, as de-

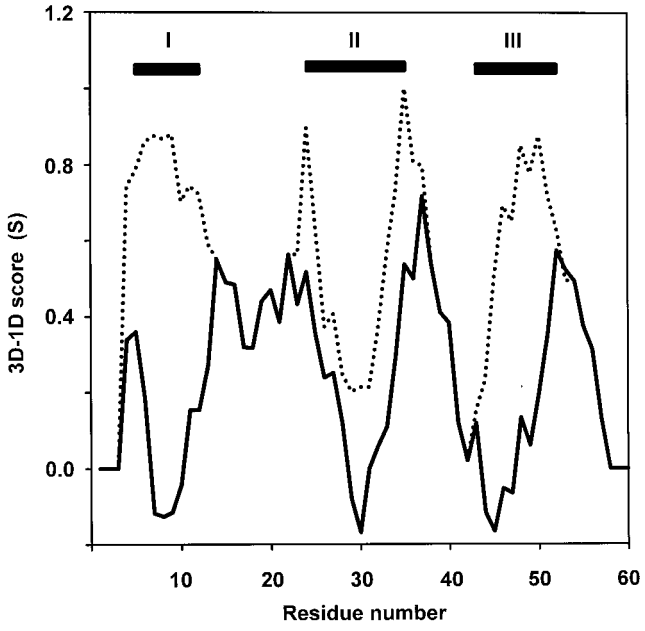

FIGURE 5 Profile window plots for a major form of cytotoxin II from *Naja oxiana* (CX2) in aqueous solution (*solid line*) and in membrane-bound state (*dotted line*). Score (*S*) is a measure of correspondence between spatial structure of CX2 and its amino acid sequence averaged inside a sliding seven-residue window. The toxin's loops are marked with roman numerals.

scribed in Methods. Overall, the results of independent techniques 1–3 point out that the putative membrane binding sites of CX2 may be delineated in the 3D structure, and all of them are located in the tips of loops I–III.

Local conformational changes in loops strongly affect the binding: minor solution form of CX2 in membrane

In water, CX2 (and other CTXs) demonstrate a certain structural "dualism," adopting two different conformations (so-called "major" and "minor" forms); the fact that seriously hampers reconstruction of 3D structure from NMR data (Jahnke et al., 1994; Dementieva et al., 1999). Major and minor solution forms of CX2 preserve the overall fold and differ in loop I: the minor form exhibits the peptide bond Val-7–Pro-8 in *cis* configuration. NMR study of CX2 in DPC micelles shows that only the major form binds to membrane-like media (Dubovskii et al., 2001). To understand why the moderate variations in conformation induce such large differences in binding, we modeled behavior of the minor form of CX2 in membrane. (Here and thereafter the membrane is uncharged.) To ensure validity of the results, two independent MC simulations were done starting from different orientations of protein with respect to the hydrophobic layer: 1) disposed in exactly the same fashion as the lowest-energy membrane-bound state described above; and 2) placed in polar phase, in arbitrary orientation with respect to the hydrophobic zone. Similar low-energy states were found in both simulations (Fig. 6 *A*). They demonstrate rather weak binding as compared to the major form: only residues Val-7 (loop I), Met-26–Val-32, Val-34 (loop II), and Leu-48 (loop III) are buried into the hydrophobic core. In the lowest-energy state, E_{np} for loops I and II are -0.43 and -7.09 kcal/mol (Fig. 3 *C*). Corresponding values of E_{int} are -1.30 and -4.44 kcal/mol. The total energy of the lowest-energy state of the CX2′ minor form in membrane is ~30 kcal/mol higher than that for the major one. Such a difference is mainly due to the solvation contribution (~25 kcal/mol), although van der Waals and torsion energies also disfavor the minor form.

A different mode of binding for S-type CTXs: cytotoxin I from *Naja atra*

CX1 belongs to the group of S-type CTXs (Chien et al., 1994) that contain Ser-28 within a putative membrane binding site near the tip of loop II, whereas P-type CTXs have Pro-31 within the same but more hydrophobic site. As seen from CX2/CX1 sequence alignment and consensus sequences for P- and S-type CTXs (Fig. 6, *bottom*), pronounced differences and most variable residues are concentrated in loop II. In comparison with the P-type CX2, the tip of loop II in CX1 is more polar due to replacements Ala-28-Ser and Ala-29-Asp. Using the same computational protocol as for the minor form of CX2, we performed MC simulations of CX1 in the presence of electrically neutral membrane. Regardless of the starting orientation, the found low-energy states have similar structure and geometry of binding (Fig. 6 *B*). Upon insertion, CX1 retains the overall spatial structure, although small conformational rearrangements are observed in loop regions, especially in loop I. Analysis of different energy terms for the lowest-energy states of CX1 in water and in membrane shows that, as for CX2, the protein's mode of binding is mainly determined by the solvation contribution. In these states CX1 is immersed in the hydrophobic region of membrane with loop I and only slightly with loop II; negative values of E_{np} are found for Ile-7, Pro-8, and Ile-9 (Fig. 3 *D*). Interactions with the interface are observed for Leu-6, Pro-8, Ile-9 (loop I), and Ile-32 (loop II). The mode of membrane binding of CX1 is quite different from that for CX2, its interaction with membrane is weaker due to considerable loss of insertion by loops II and III.

DISCUSSION

The results of computational analysis allow detailed characterization of the membrane binding motif of CTXs. The solvation model used permits assessment of protein spatial structure, geometry of membrane binding, and energetics of

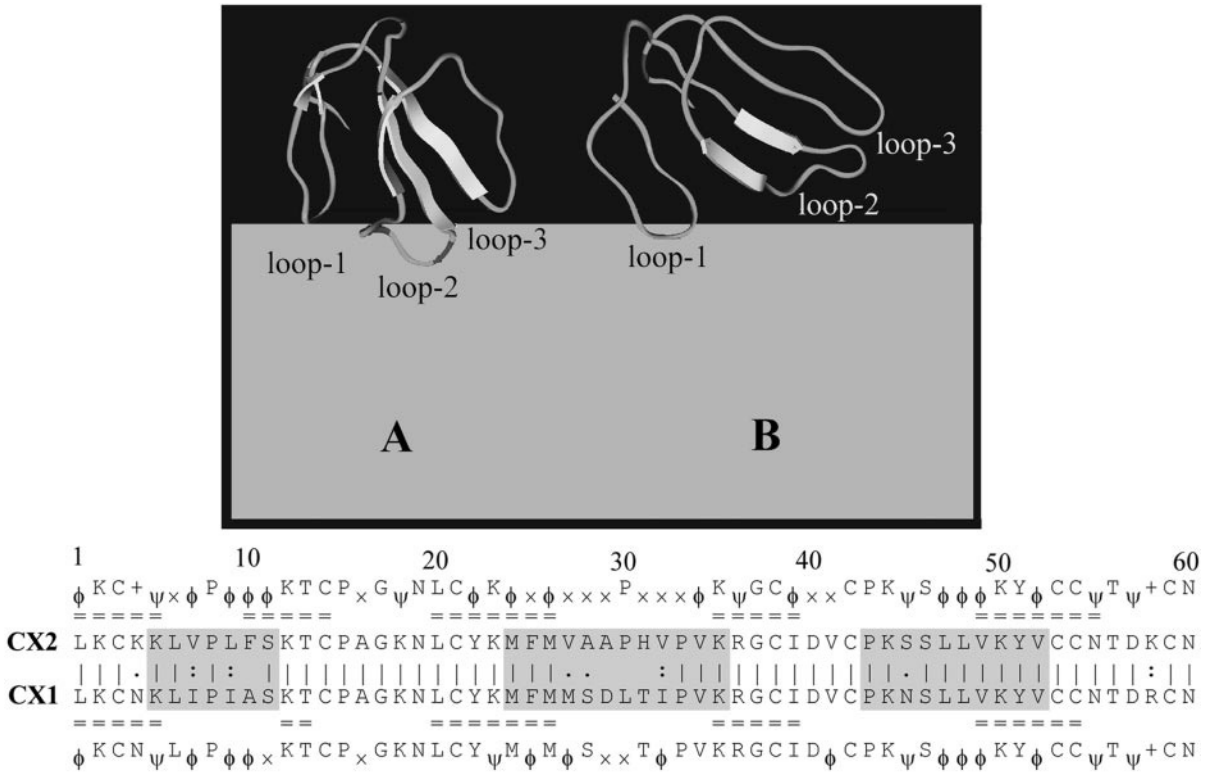

FIGURE 6 The lowest-energy states of a minor form of cytotoxin II from *Naja oxiana* (CX2, *A*) and cytotoxin I from *Naja atra* (CX1, *B*) in the presence of membrane. *Bottom:* sequence alignment between CX2 and CX1. Identical, strongly, and moderately homologous residues are marked with symbols " ", ":", and ".", respectively. Loop regions are gray-hatched. β-Strands are indicated by " =." Consensus sequences for P- and S-type cytotoxins are taken from (Chien et al., 1994). The symbols used are as follows: + for Lys and Arg; ψ, ϕ, $\times$ for polar (Lys, Arg, His, Asp, Asn, Glu, or Gln) hydrophobic and variable residues. Other details are as in legend to Fig. 2.

thousands of states (local minima) trapped in the result of exhaustive MC search. Starting with CX2 and CX1 disposed in aqueous phase, the search resulted in the most energetically favorable states, where the proteins are embedded in membrane. The toxins interact with the hydrophobic core and the membrane-water interface by means of loop regions, although CX2 strongly binds via loops I and II (and to a lesser extent with loop III), and CX1 only via loop I. The binding motif is flanked by the stretch of positive charges of Lys and Arg side chains, which are aligned just above the membrane surface. Other regions of the molecules do not enter the membrane. Thus, the states where CX2 is entirely solvated by water reveal energies higher by ~17–20 kcal/mol than those immersed in the membrane (for CX1 the corresponding value is ~6 kcal/mol). Recent estimations of the free energy cost of CX2 insertion into phospholipid vesicles based on ESR data (Dubinnyi et al., 2001) agree fairly well with the present MC results. Probably, such a reserve of energy determines functional activity of CTXs related to their partitioning from aqueous solution into cellular membranes.

Obviously, structural rearrangements in lipid bilayers induced by protein insertion are not considered in the framework of the "hydrophobic slab" model. Therefore, it can not explain membrane destabilizing activities of CTXs. However, ESR measurements reveal two different modes of CX2 binding to phospholipid vesicles (Dubinnyi et al., 2001): 1) at low concentrations monomeric CX2 is anchored via its hydrophobic loops on the membrane interface; 2) at high concentrations CX2 destroys bilayer structure. We should outline that NMR, ESR, and our modeling results are related to the aforementioned mode 1. Interestingly, such peripheral binding also precedes membrane destabilization induced by amphiphilic α-helical antimicrobial (Shai, 1999) and fusion (Dubovskii et al., 2000) peptides. Probably, this step is indispensable for subsequent lytic activity of CTXs (mode 2), which might be caused by an increase of local concentration of CTX in the membrane and accompanied by bilayer deformations, although the exact mechanism of this process and its biological role still remain unclear.

Folded membrane proteins reside in a free energy minimum determined by the interactions of the polypeptide chains with each other, the lipid hydrocarbon core, the bilayer interface, and with water. The theoretical models should properly describe the influence of membrane surrounding and yield the results consistent with the experiment (3D structure, mode of binding, membrane-induced conformational changes, hydrophobic match/mismatch, and

so forth). These criteria are satisfied in the implicit membrane model elaborated in our group and tested on TM and peripheral α-helical peptides with known 3D structure (Nolde et al., 2000). Here this model was applied to β-structural CTXs. From the structural point of view, the obtained computational results agree fairly well with the atomic scale NMR-derived model of micelle bound CX2 (Dubovskii et al., 2001). Thus, both methods yield close spatial structures of CX2 in membrane-like media. In addition, its overall 3D structure is well retained after binding to membrane: the root-mean-square deviation between C_α atoms of the calculated lowest-energy state and the NMR-derived major solution conformer (Dementieva et al., 1999), is 1.17 Å. We should note that such a structural conservativity is not always the case: membranes often induce transformations of water-soluble proteins and peptides (White and Wimley, 1999). For example, many peptides that are unordered in solution adopt α-helical or β-sheet structure in the presence of lipid bilayer, and some globular proteins are capable of inserting into membranes due to global structural rearrangements.

A wealth of experimental studies of CTXs proposed the residues at the tips of the loops which are involved in membrane/CTXs interactions (Dauplais et al., 1995; Sue et al., 1997; Sun et al., 1997; Lee at al., 1998; Dementieva et al., 1999). The experimental and simulation results on CX2 indicate that these residues do interact with membrane. Also, calculations with negatively charged membranes result in deeper insertion of CX2 (for loops II and III); a fact that agrees with the observations that CTXs bind to anionic phospholipids more strongly than to zwitterionic ones (Batenburg et al., 1985; Desormeaux et al., 1992; Carbone and Macdonald, 1996). Intuitively, this seems evident because CTXs are positively charged. However, reproducing such behavior in simulation is not straightforward because it is driven by a balance of different forces, such as electrostatic interactions and variation of E_{solv} upon insertion. The compliance obtained makes us confident that the model correctly reproduces principal trends in CTX-membrane interactions and represents a reliable approximation for modeling of toxins on both charged and neutral membrane-water interfaces. Accomplished with our previous simulations of membrane α-helices (Nolde et al., 2000; Efremov et al., 1999a,c), the computational method may be used to study partitioning of proteins with diverse folds into lipid bilayers.

Structural conservativity of the membrane-binding motif of CTXs in media of different polarity indicates that such motifs might be identified in solution or crystal structures of other proteins. Analysis of polarity properties of CX2 reveals that residues in the tips of loops I–III have unfavorable environments in water—positive values of E_{solv} and MHP, negative values of the structure-sequence compatibility score (S). In well-folded proteins, residues with such characteristics tend to change their environment to the more favorable one in the result of intermolecular interactions (Golovanov et al., 1995). In fact, insertion of CX2 into the hydrophobic core or moderately polar interfacial region of membrane results in significant "improvement" of residues' environment in the loops. Therefore, the putative membrane-binding sites might be rapidly delineated in solution or crystal structures of proteins using the proposed computational approach.

An unusual feature of the CTX-specific binding motif is the presence in membrane of backbone regions with free H-bond donors and acceptors. This distinguishes the three-finger structural pattern of CTXs from α-helices and β-barrels, which allow the hydrogen-bonding potential of the backbone to be saturated in bilayer. We assume that the energetically unfavorable exposure of non-H-bonded C═O and N—H groups to hydrophobic milieu is caused by the stability and rigidity of the CTX molecules crossed with four disulfides (Roumestand et al., 1994; Sivaraman et al., 1999, 2000). Alternatively, these groups might be involved in specific intermolecular interactions inside the membrane. In this case their possible hydrogen-bonding partners might be either headgroups of lipids or cellular receptors, putative targets of CTXs' action (Jayaraman et al., 2000).

NMR data for CX2 in DPC micelles along with the modeling results suggest that the driving forces for the toxin-membrane binding are hydrophobic and electrostatic interactions. Does the toxic activity depend only on hydrophobicity of the loops, which act as a wedge into nonpolar parts of a lipid bilayer, or also depends on their precise conformation? The simulations performed for major and minor solution forms of CX2, as well as for S-type CX1, provide an important insight into the problem. First, small conformational changes in loop I lead to dramatic changes of binding (revealed by NMR), which is well-reproduced by MC simulations. Hence, the mode of membrane binding is determined by a difference between various energy terms: even local conformational changes might disturb the balance and induce large deviations in the strength of protein-membrane interaction. Second, computer experiments on CX1 insertion demonstrate that point amino acid replacements in loop II (Fig. 6, *bottom*) also considerably affect the binding: a moderate increase of polarity in this region reduces overall membrane affinity of CTXs. This agrees with the experimental findings that P-type CTXs bind to zwitterionic (in our calculations electrically neutral) membranes stronger than S-type CTXs (Chien et al., 1994).

In the theoretical approach used we do not consider a number of important characteristics of biological membranes, such as heterogeneity of dielectric properties, chemical composition, microscopic nature of protein-lipid interactions, and so on. Some of these shortcomings might be obviated in simulations with explicit bilayers. However, most of the experimental data used to validate the theoretical approach were obtained on CTXs in micelles (including 3D structure of CX2), not in planar bilayers. Our results

reproduce main trends in CTX structure and behavior in micelles. Also, the implicit model provides a realistic description of structure and mode of membrane binding for a wide class of proteins and peptides (Nolde et al., 2000; Efremov et al., 1999a,c). We should emphasize that the objective of this study is not the determination of exact spatial structure of a protein in a lipid bilayer: taking into account aforementioned limitations, this might overestimate potentialities of the method. Our intention is to delineate (using CTXs as a new example) the main factors driving interaction of a protein with bilayers and predict its mode of membrane binding. In many cases such information is sufficient to gain deeper insight into the protein's mechanism of action and provides a basis for rationalization of experimental data. Being computationally efficient, the proposed approach permits exploration of a number of alternative scenarios that are extremely costly for experimental testing (e.g., comparative analysis of binding for wild-type and mutant proteins). Finally, the method seems to be very promising for assessment of the microscopic nature of protein-lipid interactions: low-energy states of a protein in implicit membrane found via MC search provide good starting points for subsequent long-term simulations of its behavior in fully hydrated all-atom lipid bilayers. Otherwise, modeling of protein transfer from water into explicit membrane is too computationally expensive.

Our current work is being pursued to study CX2-induced membrane destabilization. As shown by Berneche et al. (1998), in a case of α-helical peptides with lytic activity, such effects may be efficiently simulated using all-atom models of hydrated lipid bilayers. The membrane-bound states of CX2 found in the present work via MC search will be used as reasonable starting structures for explicit protein-bilayer system. We believe that the future important insight into protein-membrane interactions will be achieved by using combined, implicit, and explicit membrane models.

We are grateful to Drs. W. Braun and D. Eisenberg for providing us with the programs FANTOM and Profiles 3D, respectively. Access to computational facilities of the Joint Supercomputer Center (Moscow) is gratefully acknowledged.

This work was supported by the Russian Foundation for Basic Research (Grant 01-04-48898) and by the Ministry of Science and Technology of the Russian Federation (project 96-03-08). R.G.E. is grateful to the Science Support Foundation (Russia) for the grant awarded.

REFERENCES

Batenburg, A. M., P. E. Bougis, H. Rochat, A. J. Verkleij, and B. de Kruijff. 1985. Penetration of a cardiotoxin into cardiolipin model membranes and its implications on lipid organization. *Biochemistry.* 24: 7101–7110.

Berman, H. M., J. Westbrook, Z. Feng, G. Gilliland, T. N. Bhat, H. Weissig, I. N. Shindyalov, and P. E. Bourne. 2000. The Protein Data Bank. *Nucleic Acids Res.* 28:235–242.

Berneche, S., M. Nina, and B. Roux. 1998. Molecular dynamics simulation of melittin in a dimyristoylphosphatidylcholine bilayer membrane. *Biophys. J.* 75:1603–1618.

Bougis, P., M. Tessier, J. van Rietschoten, H. Rochat, J. F. Faucon, and J. Dufourcq. 1983. Are interactions with phospholipids responsible for pharmacological activities of cardiotoxins? *Mol. Cell. Biochem.* 55: 49–64.

Bowie, J. U., R. Lüthy, and D. Eisenberg. 1991. A method to identify protein sequences that fold into a known three-dimensional structure. *Science.* 253:164–170.

Carbone, M. A., and P. M. Macdonald. 1996. Cardiotoxin II segregates phosphatidylglycerol from mixtures with phosphatidylcholine: ^{31}P and ^{2}H NMR spectroscopic evidence. *Biochemistry.* 35:3368–3378.

Chien, K.-Y., C.-M. Chiang, Y.-C. Hseu, A. A. Vyas, G. S. Rule, and W. Wu. 1994. Two distinct types of cardiotoxin as revealed by the structure and activity relationship of their interaction with zwitterionic phospholipid dispersions. *J. Biol. Chem.* 269:14473–14483.

Dauplais, M., J. M. Neumann, S. Pinkasfeld, A. Menez, and C. Roumestand. 1995. An NMR study of the interaction of cardiotoxin gamma from *Naja nigricollis* with perdeuterated dodecylphosphocholine micelles. *Eur. J. Biochem.* 230:213–220.

Dementieva, D. V., E. V. Bocharov, and A. S. Arseniev. 1999. Two forms of cytotoxin II (cardiotoxin) from *Naja naja oxiana* in aqueous solution. Spatial structure with tightly bound water molecules. *Eur. J. Biochem.* 263:152–162.

Desormeaux, A., G. Laroche, P. Bougis, and M. Pezolet. 1992. Characterization by infrared spectroscopy of the interaction of a cardiotoxin with phosphatidic acid and with binary mixtures of phosphatidic acid and phosphatidyl choline. *Biochemistry.* 31:12173–12182.

Dubovskii, P. V., D. V. Dementieva, E. V. Bocharov, Yu. N. Utkin, and A. S. Arseniev. 2001. Membrane-binding motif of the P-type cardiotoxin. *J. Mol. Biol.* 305:137–149.

Dubovskii, P. V., H. Li, S. Takahashi, A. S. Arseniev, and K. Akasaka. 2000. Structure of an analog of fusion peptide from hemagglutinin. *Protein Sci.* 9:786–798.

Dubinnyi, M. A., P. V. Dubovskii, Yu. N. Utkin, T. N. Simonova, L. I. Barsukov, and A. S. Arseniev. 2001. An ESR study of the cytotoxin II interaction with model membranes. *Russian J. Bioorg. Chem.* 27:84–94.

Efremov, R. G., D. E. Nolde, G. Vergoten, and A. S. Arseniev. 1999b. A solvent model for simulations of peptides in bilayers. I. Membrane-promoting α-helix formation. *Biophys. J.* 76:2448–2459.

Efremov, R. G., D. E. Nolde, G. Vergoten, and A. S. Arseniev. 1999c. A solvent model for simulations of peptides in bilayers. II. Membrane-spanning alpha-helices. *Biophys. J.* 76:2460–2471.

Efremov, R. G., D. E. Nolde, P. E. Volynsky, A. A. Chernyavsky, P. V. Dubovskii, and A. S. Arseniev. 1999a. Factors important for fusogenic activity of peptides: molecular modeling study of analogs of fusion peptide of influenza virus hemagglutinin. *FEBS Lett.* 462:205–210.

Efremov, R. G., and G. Vergoten. 1995. Hydrophobic nature of membrane-spanning α-helical peptides as revealed by Monte Carlo simulations and molecular hydrophobicity potential analysis. *J. Phys. Chem.* 99: 10658–10666.

Forrest, L. R., and M. S. Sansom. 2000. Membrane simulations: bigger and better? *Curr. Opin. Struct. Biol.* 10:174–181.

Gatineau, E., M. Takechi, F. Bouet, P. Mansuelle, H. Rochat, A. L. Harvey, T. Montenay-Garestier, and A. Menez. 1990. Delineation of the functional site of a snake venom cardiotoxin: preparation, structure, and function of monoacetylated derivatives. *Biochemistry.* 29:6480–6489.

Golovanov, A. P., R. G. Efremov, V. A. Jaravine, G. Vergoten, and A. S. Arseniev. 1995. Amino acid residue: is it structural or functional? *FEBS Lett.* 375:162–166.

Jahnke, W., D. F. Mierke, L. Beress, and H. Kessler. 1994. Structure of cobra cardiotoxin CTXI as derived from nuclear magnetic resonance spectroscopy and distance geometry calculations. *J. Mol. Biol.* 240: 445–458.

Jayaraman, G., T. K. S. Kumar, C.-C. Tsai, S. Srisailam, S.-H. Chou, and C.-L. Ho. 2000. Elucidation of the solution structure of cardiotoxin analogue V from the Taiwan cobra (*Naja naja atra*)—identification of

structural features important for the lethal action of snake venom cardiotoxins. *Protein Sci.* 9:637–646

Kabsch, W., and C. Sander. 1983. Dictionary of protein secondary structure: pattern recognition of hydrogen-bonded and geometrical features. *Biopolymers.* 22:2577–2637.

Koradi, R., M. Billeter, and K. Wüthrich. 1996. MOLMOL: a program for display and analysis of macromolecular structures. *J. Mol. Graphics.* 14:51–55.

Kumar, T. K. S., G. Jayaraman, C. S. Lee, A. I. Arunkumar, T. Sivaraman, D. Samuel, and C. Yu. 1997. Snake venom cardiotoxins: structure, dynamics, function and folding. *J. Biomol. Struct. Dyn.* 15:431–463.

La Rocca, P., P. C. Biggin, D. P. Tieleman, and M. S. P. Sansom. 1999. Simulation studies of the interaction of antimicrobial peptides and lipid bilayers. *Biochim. Biophys. Acta.* 1462:185–200.

Lee, C. S., T. K. Kumar, L. Y. Lian, J. W. Cheng, and C. Yu. 1998. Main-chain dynamics of cardiotoxin II from Taiwan cobra (*Naja naja atra*) as studied by carbon-13 NMR at natural abundance: delineation of the role of functionally important residues. *Biochemistry.* 37:155–164.

Metropolis, N., A. W. Rosenbluth, A. H. Teller, and E. Teller. 1953. Equation of state calculations for fast computing machines. *J. Chem. Phys.* 21:1087–1092.

Némethy, G., M. S. Pottle, and H. A. Scheraga. 1983. Energy parameters in polypeptides. 9. Updating of geometrical parameters, nonbonded interactions, and hydrogen bond interactions for the naturally occurring amino acids. *J. Phys. Chem.* 87:1883–1887.

Nolde, D. E., P. E. Volynsky, A. S. Arseniev, and R. G. Efremov. 2000. Modeling of peptides and proteins in a membrane environment. I. A solvation model mimicking a lipid bilayer. *Russian J. Bioorg. Chem.* 26:115–124.

Roumestand, C., B. Gilquin, O. Tremeau, E. Gatineau, L. Mouawad, A. Menez, and F. Toma. 1994. Proton NMR studies of the structural and dynamical effect of chemical modification of a single aromatic side-chain in a snake cardiotoxin. Relation to the structure of the putative binding site and the cytolytic activity of the toxin. *J. Mol. Biol.* 243: 719–735.

Shai, Y. 1999. Mechanism of the binding, insertion and destabilization of phospholipid bilayer membranes by alpha-helical antimicrobial and cell non-selective membrane-lytic peptides. *Biochim. Biophys. Acta.* 1462: 55–70.

Sivaraman, T., T. K. Kumar, K. W. Hung, and C. Yu. 2000. Comparison of the structural stability of two homologous toxins isolated from the Taiwan cobra (*Naja naja atra*) venom. *Biochemistry.* 39:8705–8710.

Sivaraman, T., T. K. Kumar, and C. Yu. 1999. Investigation of the structural stability of cardiotoxin analogue III from the Taiwan cobra by hydrogen-deuterium exchange kinetics. *Biochemistry.* 38:9899–9905.

Sue, S.-C., P. K. Rajan, T.-S. Chen, C.-H. Hsieh, and W. Wu. 1997. Action of Taiwan cobra cardiotoxin on membranes: binding modes of a beta-sheet polypeptide with phosphatidylcholine bilayers. *Biochemistry.* 36: 9826–9836.

Sun, Y. J., W. G. Wu, C. M. Chiang, A. Y. Hsin, and C. D. Hsiao. 1997. Crystal structure of cardiotoxin V from Taiwan cobra venom: pH-dependent conformational change and a novel membrane-binding motif identified in the three-finger loops of P-type cardiotoxin. *Biochemistry.* 36:2403–2413.

Tieleman, D. P., H. J. Berendsen, and M. S. Sansom. 2001. Voltage-dependent insertion of alamethicin at phospholipid/water and octane/water interfaces. *Biophys. J.* 80:331–346.

Vincent, J. P., M. Balerna, and M. Lazdunski. 1978. Properties of association of cardiotoxin with lipid vesicles and natural membranes. A fluorescence study. *FEBS Lett.* 85:103–108.

von Freyberg, B., and W. Braun. 1991. Efficient search for all low energy conformations of polypeptides by Monte Carlo methods. *J. Comp. Chem.* 12:1065–1076.

White, S. H., and W. C. Wimley. 1999. Membrane protein folding and stability: physical principles. *Annu. Rev. Biophys. Biomol. Struct.* 28: 319–365.